Sun *et al*. *Intell Robot* 2023;3(3):257-73
DOI: 10.20517/ir.2023.17

Intelligence & Robotics

Research Article

Open Access

State-sensitive event-triggered path following control of autonomous ground vehicles

Hong-Tao Sun[1], Jinming Huang[1], Zhi Chen[2], Zhiwen Wang[3]

[1]College of Engineering, Qufu Normal University, Qufu 273165, Shandong, China.
[2]Department of Automation, School of Mechatronic Engineering and Automation, Shanghai University, Shanghai 200444, China.
[3]College of Electrical and Information Engineering, Lanzhou University of Technology, Lanzhou 730050, Gansu, China.

Correspondence to: Prof. Jinming Huang, College of Engineering, Qufu Normal University, No. 80, Yantai Road, Rizhao 276826, Shandong, China. E-mail: huangjm@qfnu.edu.cn

How to cite this article: Sun HT, Huang J, Chen Z, Wang Z. State-sensitive event-triggered path following control of autonomous ground vehicles. *Intell Robot* 2023;3(3):257-73. http://dx.doi.org/10.20517/ir.2023.17

Received: 10 Mar 2023 **First Decision:** 29 May 2023 **Revised:** 2 Jun 2023 **Accepted:** 12 Jun 2023 **Published:** 20 Jul 2023

Academic Editor: Simon X. Yang, Hongtian Chen **Copy Editor:** Yanbin Bai **Production Editor:** Yanbin Bai

Abstract

This paper investigates an improved event-triggered control based on the perception of state measurement for path following control of autonomous ground vehicles. Firstly, in order to regulate the event-triggered thresholds dynamically, a barrier-like function is first used to develop such a novel state-sensitive event-triggered communication (SS-ETC) scheme. Different from the existing variable-threshold ETC schemes, the proposed SS-ETC incorporates the state measurements directly in the event threshold adjustment, eliminating the need for additional terms or dynamics introduced in previous works. Secondly, the networked path following control modeling issues, which include both physical dynamics and the SS-ETC scheme, are characterized by the input delay approach. The controller design method is well derived, ensuring the preservation of input-to-state stability of the path following control system. The main advantage of this paper lies in the proposed SS-ETC, which shows a better trade-off between control and communication. Finally, several simulation experiments are conducted to verify the effectiveness of the proposed event-triggered control scheme.

Keywords: Networked control systems, event-triggered scheme, autonomous ground vehicles, path following control

1.INTRODUCTION

In the past few decades, the autonomous ground vehicles (AGVs) are rapidly developing because of their wide applications in military and civilian fields[1–4]. Vehicle motion control, as the main function for fulfilling tasks, has become increasingly important in the design of AGVs. Since the sensors, controllers, and actuators are interconnected through communication networks, AGVs have evolved into typical networked control systems (NCSs)[5,6]. Due to the limited bandwidth in-vehicle network, the network-induced delays and packet dropouts impose additional constraints on the control loop in AGVs. Therefore, the control issues that consider information exchange schemes have gained popularity in designing of AGVs[6–9].

Path following control, which involves ensuring that a vehicle tracks the desired path with zero-steady state error, is a fundamental ability for AGVs[10,11]. It is worth noting that the GPS, which is used for positioning and navigation, is important to the path following control of AGVs. Up to now, it should be mentioned that the advent of shared communication brings some new challenges due to the networked integration of path following control. Therefore, the path following control needs to consider not only the in-vehicle communication network but also the out-communication network. In a traditional way, although many efforts have been dedicated to developing path following control strategies, only a few of them can cope with time delays or packet dropouts caused by networks due to the low networked integrations for AGVs[12,13]. Various control strategies have been developed to deal with such network-introduced difficulties, such as fuzzy control[14], MPC algorithm[8], robust control method[9,15,16], and adaptive control strategy[17]. However, the results of those methods show some conservations in communication scheduling. Based on the observation of existing works, there is still much room for further research on the co-design of control and communication for networked AGVs. This motivated us to study event-triggered path following control of AGVs.

To address the co-design issues of path following control and communication, the event-triggered communication (ETC) scheme, which transmits its measurement data only according to control requirements, has been proposed and received much attention from the control community. Compared to traditional time-triggered communication schemes, the ETC scheme is efficient in reducing communication frequency, thereby helping to avoid network congestion in in-vehicle networks. In addition, a larger communication interval can provide an extra time slot for scheduling vehicles among AGVs while preserving control performance[18]. However, the event-triggered control scheme of path following control in AGVs is considered just in a few of works[19–22], making it meaningful to develop ETC schemes specifically in path following control for AGVs. Furthermore, since functional safety is very important to the motion control of AGVs, a more intelligent ETC scheme should be well developed for path following control. In fact, ETC schemes have been extensively investigated in NCSs due to their resource-saving nature[23,24] and the references therein. Up to now, several novel ETC schemes have been developed to solve the problems arising from networks. For example, the adaptive ETC scheme that depended on state gradient is proposed to adjust the event threshold in[25], while a dynamic ETC scheme that introduces an additional positive term in the traditional ETC scheme is presented in[26]. Resilient ETC schemes are also proposed in[27,28] to deal with denial of service attacks, and learning-based ETC schemes are developed to cope with deception attacks in[19]. Furthermore, a memory-based ETC scheme is developed to improve control performance in[29]. Although the existing works on event-trigged control strategies show a flexible capacity to adjust transmission frequency, such previous works on the design of advanced ETC need extra terms or dynamics to adjust the event-triggered parameters rather than the parameters themselves. Therefore, these adjustment strategies of event-triggered threshold are blind to state perception, which splits the co-design of communication and control to some extent. In addition, due to the limited bandwidth for the in-vehicle communication network and limited capacity of calculation for the electronic control unit (ECU), using ETC to reduce communication and control burden is highly advantageous for path following control of AGVs.

Due to the limitation of the previous works, the state-measurement-based event-triggered control scheme is

first developed to make a trade-off between communication efficiency and control performance. The proposed scheme, known as the state-sensitive (SS)-ETC scheme, incorporates the state measurement directly into the adjustment of event-triggered threshold dynamically. The convergence of the dynamic event-triggered thresholds is also removed while the stability of the path following control is not destroyed. The main contributions of this paper can be summarized as follows:

- The SS-ETC scheme is developed to adaptively adjust the event threshold. A barrier-like function is first introduced to indicate the SS-ETC scheme for path following control of AGVs. Compared to the static ETC scheme[30] with a fixed event-triggered parameter, the proposed SS-ETC can adjust the event-triggered threshold dynamically by introducing such a barrier-like function. Importantly, there is no need to introduce extra terms or dynamics when adjusting the event-triggered threshold. This is very different from the previous works, such as adaptive ETC scheme[25] and dynamic ETC scheme[26].
- The state measurement will directly contribute to the adjustment of an event-triggered threshold. Unlike the separate descriptions for physical dynamics and communication intervals in previous works[27,28], the dynamics of plant and communication scheme are intergraded in a uniform way. This approach gives a clearer presentation on stability properties and communication behavior. In addition, the proposed SS-ETC scheme is based on the sampled-data framework, which is different from the continuous one proposed by[31].
- The stability of the path following control of AGV is naturally guaranteed by the proposed SS-ETC scheme. With the proposed SS-ETC scheme, all the event-triggered thresholds can be naturally suppressed within a stability region. This approach provides a more flexible way to the co-design of communication and control in path following control of AGV.

Compared to the previous works, the proposed SS-ETC scheme, based on state perception, shows a higher level of adaptiveness on threshold adjustment in order to improve the functional safety of AGVs.

The remainder of this paper is organized as follows: Section II gives a more detailed description on the proposed SS-ETC and NCS modeling for path following control of AGVs. Section III presents the main results of this work, including the stability analysis and controller design under the proposed SS-ETC. In section IV, simulation results, which were conducted on a networked path following control of AGVs, are shown to verify the proposed theoretical results. Finally, section V concludes this paper.

To the end of this section, some physical meanings of related self-steering control of autonomous vehicles (AVs) are given below Table 1.

2. PROBLEM FORMULATION

In this section, we first present the networked path following control modeling. Then, the SS-ETC scheme is proposed to dynamically adjust the event-triggered parameter. At last, the path following control modeling of AGVs under the proposed SS-ETC scheme is established.

2.1. Networked path following control framework

A networked path following control of AVs can be classified as a typical NCS, where all the measurements are transmitted over a CAN bus and GPS network, among others. The control actions are calculated by an ECU. To optimize the utilization of communication and computation resources, this paper introduces the SS-ETC unit. The introduction of the SS-ETC unit aims to address the following two problems:

- Under the conditions of resource constraints of in-and-out vehicle networks, the SS-ETC unit should regulate its communication behavior to realize a more efficient utilization of resources.
- Considering the control requirements of the path following control, the SS-ETC unit must ensure the stability of the path following control of AVs under resource-constrained environments.

Table 1. Physical meanings in path following control

Parameter	Physical meaning
m	the mass of vehicle
F_{yf}	the lateral forces of the front tire
F_{yr}	the lateral forces of the rear tire
α_f	the tire slip angle of the front tire
α_r	the tire slip angle of the rear tire
β	the vehicle sideslip angle
I_z	the yaw inertia of the vehicle
l_f	the center of gravity of the vehicle to the front wheel axis
l_r	the center of gravity of the vehicle to the rear wheel axis
C_f	the front tire cornering stiffness
C_r	the rear tire cornering stiffness
e	the lateral offset from the vehicle center of gravity to the closest T on the desired path
ψ	the error between the actual heading angle ψ_h and the desired heading angle ψ_d
r	the yaw rare of the vehicle with $\dot{\psi}_h = r$
v_x	the longitudinal velocity of the vehicle
v_y	the lateral velocity of the vehicle
δ_f	the front-wheel steering angle
σ	the curvilinear coordinate of point T along the path from an initial position predefined
$\rho(\sigma)$	the curvature of the desired path at the point T.

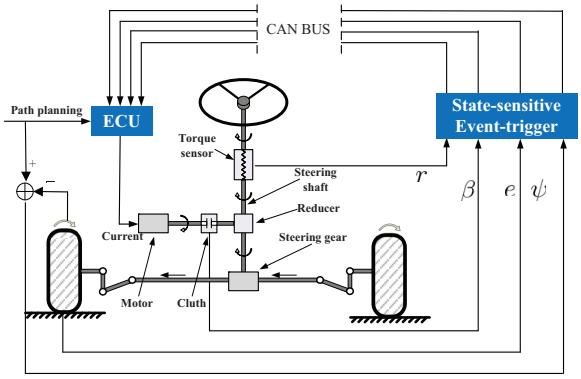

Figure 1. Path following control diagram with SS-ETC scheme.

The framework of the networked path following control is shown in Figure 1. Then, the mathematical modeling of path following control of AVs is given as follows

$$\begin{cases} \dot{e} = v_x\beta + v_x\psi + d_1 \\ \dot{\psi} = r - \rho(\sigma)v_x \\ \dot{\beta} = a_{11}\beta + a_{12}r + b_1\delta_f + d_2 \\ \dot{r} = a_{21}\beta + a_{22}r + b_2\delta_f + d_3. \end{cases} \tag{1}$$

with

$a_{11} = -\frac{(C_f+C_r)}{mv_x}, a_{12} = -(1 + \frac{(l_fC_f-l_rC_r)}{mv_x^2}),$

$a_{21} = \frac{(l_rC_r-l_fC_f)}{I_z}, a_{22} = -(\frac{(l_f^2C_f+l_r^2C_r)}{v_xI_z}),$

$b_1 = \frac{C_f}{mv_x}, b_2 = \frac{l_fC_f}{I_z}.$

Further, define the state vector $x(t) = [e, \psi, \beta, r]^T$, the control input $u(t) = \delta_f$, the state-space form of the path following model[32] of AVs can be given as follows

$$\dot{x}(t) = Ax(t) + Bu(t) + w(t) \tag{2}$$

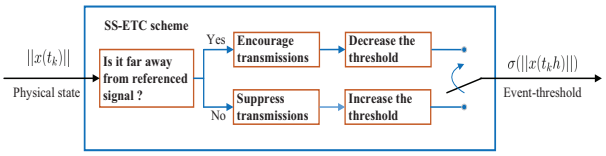

Figure 2. The basic idea of the SS-ETC.

where

$$A = \begin{bmatrix} 0 & v_x & v_x & 0 \\ 0 & 0 & 0 & 1 \\ 0 & 0 & a_{11} & a_{12} \\ 0 & 0 & a_{21} & a_{22} \end{bmatrix}, B = \begin{bmatrix} 0 \\ 0 \\ b_1 \\ b_2 \end{bmatrix}, w(t) = \begin{bmatrix} d_1 \\ -\rho(\sigma)v_x \\ d_2 \\ d_3 \end{bmatrix}$$

Here, the disturbance $w(t) = [d_1, -\rho(\sigma)v_x, d_2, d_3]^T$ with modeling errors d_1, d_2, and d_3.

For the purpose of achieving a better understanding of the proposed SS-ETC framework, the following general assumptions are given first.

Assumption 1 *The sensors are time triggered with a fixed sampling period h. Then, the sampling set $\mathbb{S}_1 = \{0, h, 2h, \cdots, kh\}$ is assumed for all $k \in \mathbb{N}$ under a sampled-data framework.*

Assumption 2 *Under the ETC scheme, not all the sampled data would be transmitted. Therefore, one can assume that the set of successfully transmitted samples is $\mathbb{S}_2 = \{0, t_1 h, t_2 h, \cdots, t_k h\}$. Obviously, $\mathbb{S}_2 \subseteq \mathbb{S}_1$.*

Assumption 3 *The controllers and actuators are event-triggered. Then the control input at the actuator is generated by a zero-order holder (ZOH) with its holding interval $t \in [t_k h + \tau_{t_k}, t_{k+1} h + \tau_{t_{k+1}})$. Here, τ_{t_k} is the transmission delay.*

Remark 1 *The main difference between $\mathbb{S}_1$ and $\mathbb{S}_2$ lies in the fact that not all the sampled data would be transmitted for the ETC scheme. In fact, if $\mathbb{S}_1 = \mathbb{S}_2$, it means that all sampled data are transmitted, and the event-triggered transmission becomes a time-triggered transmission for Assumption. 2.*

2.2. SS-ETC scheme

The basic idea of the proposed SS-ETC scheme, which adjusts its event-triggered threshold according to the received state measurement, is captured by Figure 2.

The properties of the SS-ETC can be attributed to the following two cases:

- When a larger state measurement $||x(t_k h)||$ is received, the SS-ETC scheme deems that the physical system becomes unstable, and it would encourage transmissions to stabilize the physical system with a higher control frequency. Then a lower event-triggered is adopted.
- When a smaller state measurement $||x(t_k h)||$ is received, the SS-ETC scheme deems that the physical system is stable, and some unnecessary transmissions can be reduced. Then an upper event-triggered threshold is maintained.

In order to highlight the SS-ETC scheme, we begin by introducing the following barrier-like function:

$$f(x) = \frac{a}{x + b} \tag{3}$$

where a and b are given positive constants, and $x \geq 0$ is an independent variable.

From (3), the following facts can be easily obtained:

- The upper bound of $f(x)$ is $\frac{a}{b}$, while $x = 0$.
- A larger x leads to a smaller $f(x)$ and vice versa. In addition, when $x \to \infty$, $f(x) \to 0$.
- b is used to avoid zero in the denominator.

Since the ETC is an error-oriented communication scheme, then $\varsigma(i_k h)$ is generally defined as the state error between the current sampling instant and the latest transmitted sampling instant, i.e.,

$$\varsigma(i_k h) = x(i_k h) - x(t_k h) \tag{4}$$

with $i_k h = t_k h + \ell h$, $\ell \in \mathbb{N}$.

Motivated by (3), the SS-ETC scheme described in Figure 1 is designed as

$$t_{k+1}h = t_k h + \min_{\ell}\{\ell h | \varsigma^T(i_k h)\Phi\varsigma(i_k h) \geq \frac{\sigma_\epsilon}{||x(t_k h)|| + \epsilon}\mathcal{X}(t_k)\} \tag{5}$$

where $\mathcal{X}(t_k) = x^T(t_k h)\Phi x(t_k h)$. $\epsilon > 0$ is a given constant, σ_ϵ is a positive event-triggered parameter related to ϵ, and Φ is a positive definite matrix to be designed.

The event defined by $\frac{\sigma_\epsilon}{||x(t_k h)||+\epsilon}\mathcal{X}(t_k)$ is important to the transmission under the ETC scheme. It is worth noting that the existing parameter ϵ is used to avoid zero in the denominator when one wants to design a meaningful event-triggered scheme (5). In addition, once the parameter ϵ is selected, the corresponding event-triggered parameter σ_ϵ can be designed.

Remark 2 *In fact, the threshold value is important to make a trade-off between control performance and communication efficiency. The basics of the event design are to guarantee the stability of the controlled systems. But it is not easy to seek the best threshold because of time-varying requirements on control performance and communication efficiency. Thus, one can design dynamic ETC schemes or adaptive ETC schemes in order to achieve a better trade-off between control performance and communication efficiency.*

Remark 3 *From the SS-ETC (5), a dynamic event threshold is well characterized by* $\frac{\sigma_\epsilon}{||x(t_k h)||+\epsilon}$*, which is related to the parameters* ϵ*,* σ_ϵ*, and* $||x(t_k h)||$*. Based on the established SS-ETC scheme, we can arrive at*

- *The pair* (ϵ,σ_ϵ) *gives the basis of the event-triggered parameter design while preserving the input-to-state stability (ISS). For a different* ϵ*, one can derive a corresponding* σ_ϵ *to guarantee the existing of the controller* K*;*
- *The* $\frac{\sigma_\epsilon}{\epsilon}$ *supplies a upper bound of event-triggered parameter when* $||x(t_k h)|| = 0$*. This indicates that a lower transmission frequency is expected while the stability of the studied NCS is guaranteed;*
- *The event-triggered threshold is dynamically adjusted according to the latest available measurement* $||x(t_k h)||$*, directly.*

Thus, the main advantages of the proposed SS-ETC lie in that: 1) by comparing adaptive ETC proposed in[25]*, the lower bound of the event-triggered* σ_m *is not needed for the proposed SS-ETC (5); 2) by comparing the dynamic ETC scheme*[26]*, the extra term* $\eta(t)$*, which is used to adjust the event threshold, is not necessary for the proposed SS-ETC (5); 3) It is clear that the thresholds of the proposed SS-ETC scheme (5) are always arrested in a stability region while threshold adjusting.*

Therefore, the proposed SS-ETC (5) will make a trade-off between communication efficiency and control performance while the desired stability is guaranteed.

2.3. Path following control modeling under SS-ETC scheme

Under the above assumptions, the actual control actions based on (2) with a fixed controller can be represented as follows:

$$\begin{cases} \dot{x}(t) = Ax(t) + Bu(t) + w(t) \\ u(t) = Kx(t_k h), t \in [t_k h + \tau_{t_k}, t_{k+1} h + \tau_{t_{k+1}}) \end{cases} \tag{6}$$

where K is the cloud controller gain to be designed.

In the following, the divisions of the sampling-like intervals for $[t_k h + \tau_k, t_{k+1} h + \tau_{k+1})$ are presented according to [30]. Assume that

$$\Omega = \cup_{\ell=0}^{t_{k+1}-t_k-1} \Omega_\ell$$

where $\Omega_\ell = [i_k h + \tau_{i_k}, i_k h + h + \tau_{i_k+1})$ with $i_k h = t_k h + \ell h$.

By defining

$$\tau(t) = t - i_k h \tag{7}$$

for all $t \in \Omega_\ell$, then the piece-wise function satisfying $\dot{\tau}(t) = 1$, and

$$0 \leq \tau_m = \min\{\tau_{t_k}, \tau_{t_{k+1}}\} \leq h + \max\{\tau_{t_k, \tau_{k+1}}\} = \tau_M.$$

Therefore, the control action of (6) can be represented as

$$u(t) = K(x(t - \tau(t)) - \varsigma(i_k h)) \tag{8}$$

by combing (4) and (7).

Further, the NCS modeling under SS-ETC (5) is described as

$$\begin{cases} \dot{x}(t) = Ax(t) + BK(x(t - \tau(t)) - \varsigma(i_k h)) + w(t) \\ \text{subjects to:} \\ \varsigma^T(i_k h)\Phi\varsigma(i_k h) \leq \dfrac{\sigma_\epsilon}{||x(t_k h)|| + \epsilon} \mathcal{X}(t_k) \end{cases} \tag{9}$$

where the detailed meaning of parameters is given by the aforementioned equation (5). Here, the initial state of the $x(t)$ can be defined as $x(t_0)$ for $t \in [t_0 - \tau_M, t_0)$.

Remark 4 *In fact, (9) gives a more compact form of the event-triggered control for the NCS. From (9), it is clear that the stability of the closed loop dynamics now depends on the control update rule through $\varsigma(i_k h)$. If the SS-ETC scheme, where the event-triggered condition given in the below equation of (9), keeps $\varsigma(i_k h)$ in a small sense, the stability of the studied dynamics would not be destroyed. This is the reason that one can stabilize (9) with a variable-threshold ETC scheme with the same controller K.*

By using the proposed SS-ETC scheme (5), this paper attempts to pursue the ISS analysis and the controller synthesis for the NCS (9) while the following objectives are achieved.

Definition 1 *The NCS (8) resulting in (5) is said to be input-to-state stable (ISS), if there exist a $\mathcal{KL}$-function ψ and $\mathcal{K}_\infty$-function ϕ such that*

$$||x(t)|| \leq \psi(||x(t_0)||, t) + \phi(||w(t)||_\infty) \tag{10}$$

for all $w(t) \in \mathcal{L}_\infty$.

3. MAIN RESULTS

In this section, the stability analysis and input to state stabilization issues are conducted with Lyapunov theory. In addition, the co-design algorithm is also presented at the end of this section.

For facilitating the proofs in the following sections, the following useful lemmas, which play important roles in our derivations, are presented first.

Lemma 1 [33] *For any positive definite matrix* $R \in \mathbb{R}^{n\times n}$ *with* $R = R^T$, *a scalar* $\mu > 0$ *and a vector function* $\dot{x} : [-\mu, 0] \to \mathbb{R}^n$ *such that the following integration inequality is well defined, i.e.,*

$$-\eta \int_{t-\eta}^{t} \dot{x}^T(s) R \dot{x}(s) ds \le -\xi^T(t) \begin{bmatrix} R & -R \\ -R & R \end{bmatrix} \xi(t) \tag{11}$$

where $\xi^T(t) = \begin{bmatrix} x(t) & x(t-\eta) \end{bmatrix}$.

Lemma 2 [34] *For any matrix* $R > 0$, $\begin{bmatrix} R & S \\ S^T & R \end{bmatrix} > 0$, *scalars* $-\eta_2 \le \eta(t) \le -\eta_1$, *and a vector function* $\dot{x} : [-\eta_2, -\eta_1] \to \mathbb{R}^n$ *such that the following integration inequality is well defined, i.e.,*

$$\begin{aligned} -(\eta_2 - \eta_1) \int_{t-\eta_2}^{t-\eta_1} \dot{x}^T(s) R \dot{x}(s) ds \le \\ -\zeta^T \begin{bmatrix} R & S-R & -S \\ * & 2R-S-S^T & S-R \\ * & * & R \end{bmatrix} \zeta(t) \end{aligned} \tag{12}$$

where $\zeta^T(t) = \begin{bmatrix} x(t-\eta_1) & x(t-\eta(t)) & x(t-\eta_2) \end{bmatrix}$.

3.1. Stability analysis

Theorem 1 *For some positive scalars* ϵ, σ_ϵ, τ_m, τ_M $(\tau_m \le \tau_M)$, α, ς, *and matrix* K, *if there exist real symmetric positive definite matrices* P, Q_i, R_i $(i \in \{1, 2\})$ *and arbitrary matrices* S *for such that the follow inequalities hold*

$$\Pi = \begin{bmatrix} \Pi_{11} & \Pi_{12} \\ * & \Pi_{22} \end{bmatrix} < 0, \quad \begin{bmatrix} R_2 & S \\ * & R_2 \end{bmatrix} > 0 \tag{13}$$

where

$\Pi_{11} = [(1,1) = A^T P + PA + 2\alpha P + Q_1 - e^{-2\alpha\tau_m} R_1,$
$(1,2) = e^{-2\alpha\tau_m} R_1, (1,3) = PBK, (1,5) = -PBK,$
$(1,6) = PF,$
$(2,2) = e^{-2\alpha\tau_m}(Q_2 - R_1 - Q_1) - e^{-2\alpha\tau_M} R_2, \quad (2,3) = e^{-2\alpha\tau_M}(R_2 - S), (2,4) = e^{-2\alpha\tau_M} S,$
$(3,3) = e^{-2\alpha\tau_M}(S + S^T - 2R_2) + \frac{\sigma_\epsilon}{\epsilon}\Phi,$
$(3,4) = e^{-2\alpha\tau_M}(R_2 - S), (3,5) = -\frac{\sigma_\epsilon}{\epsilon}\Phi,$
$(4,4) = e^{-2\alpha\tau_M}(-R_2 - Q_2), (5,5) = \frac{\sigma_\epsilon}{\epsilon}\Phi - \Phi,$
$(6,6) = -\varsigma].$
$\Pi_{12} = [\tau_m R_1 \Gamma, (\tau_M - \tau_m) R_2 \Gamma].$
$\Pi_{22} = diag[-R_1, -R_2],$
$\Gamma^T = [A, 0, BK, 0, -BK, F].$

Then, the NCS (9) under SS-ETC scheme (5) is ISS.

Proof: See Appendix.

From the proof of Theorem 1, it is clear that the convergence speed of the proposed event-triggered control algorithm is indicated by the parameter α. Namely, for a given convergence speed α, if a solution exists for the LMIs (13) under the proposed SS-ETC scheme (5), the convergence speed α is achieved by the designed controller K.

Remark 5 *Compared to the static ETC scheme proposed in[30] and adaptive ETC scheme[20], the SS parameter ϵ is introduced during the proof of the stability analysis. Obviously, the different event-triggered parameter σ_ϵ can be obtained by a different SS parameter ϵ. Thus, $\sigma_\epsilon \in [0,1)$ is removed during the design of the corresponding event-triggered parameter while introducing an appropriate ϵ. By combing Remark 4, one can see that the $\frac{\sigma_\epsilon}{\epsilon}$ supplies the upper bound of the event-triggered threshold. Thus, any event-triggered thresholds less than $\frac{\sigma_\epsilon}{\epsilon}$ would not destroy the stability property of the physical systems.*

3.2. Controller design with its algorithm

Theorem 2 *For some positive scalars ϵ, σ_ϵ, τ_m, τ_M ($\tau_m \le \tau_M$), α, ς, if there exist real symmetric positive definite matrices X, $\overline{Q}_i$, $\overline{R}_i$ ($i \in \{1,2\}$) and arbitrary matrices $\overline{S}$ for such that the follow inequalities hold*

$$\overline{\Pi} = \begin{bmatrix} \overline{\Pi}_{11} & \overline{\Pi}_{12} \\ * & \overline{\Pi}_{22} \end{bmatrix} < 0, \quad \begin{bmatrix} \overline{R}_2 & \overline{S} \\ * & \overline{R}_2 \end{bmatrix} > 0 \tag{14}$$

where

$$\begin{aligned}
\overline{\Pi}_{11} = [&(1,1) = XA^T + AX + 2\alpha X + \overline{Q}_1 - e^{-2\alpha\tau_m}\overline{R}_1,\\
&(1,2) = e^{-2\alpha\tau_m}\overline{R}_1, (1,3) = BY, (1,5) = -BY,\\
&(1,6) = F,\\
&(2,2) = e^{-2\alpha\tau_m}(\overline{Q}_2 - \overline{R}_1 - \overline{Q}_1) - e^{-2\alpha\tau_M}\overline{R}_2, \qquad (2,3) = e^{-2\alpha\tau_M}(\overline{R}_2 - \overline{S}), (2,4) = e^{-2\alpha\tau_M}\overline{S},\\
&(3,3) = e^{-2\alpha\tau_M}(\overline{S} + \overline{S}^T - 2\overline{R}_2) + \tfrac{\sigma_\epsilon}{\epsilon}\overline{\Phi},\\
&(3,4) = e^{-2\alpha\tau_M}(\overline{R}_2 - \overline{S}), (3,5) = -\tfrac{\sigma_\epsilon}{\epsilon}\overline{\Phi},\\
&(4,4) = e^{-2\alpha\tau_M}(-\overline{R}_2 - \overline{Q}_2), (5,5) = \tfrac{\sigma_\epsilon}{\epsilon}\overline{\Phi} - \overline{\Phi},\\
&(6,6) = -\varsigma].\\
\Pi_{12} = [&\tau_m\overline{R}_1\Gamma, (\tau_M - \tau_m)\overline{R}_2\Gamma].\\
\Pi_{22} = &diag[X - 2\overline{R}_1, X - 2\overline{R}_2],\\
\Gamma^T \quad = &[AX, 0, BY, 0, -BY, F].
\end{aligned}$$

Then, the NCS (9) under SS-ETC scheme (5) can be stabilized by the controller $K = YX^{-1}$ while ISS is preserved.

Proof: The proof of this section is based on Theorem 1. By defining $X = P^{-1}$, $\overline{Q}_i = XQ_iX^T$, $\overline{R}_i = XR_iX^T$, $\overline{S} = XSX^T$, $\overline{\Phi} = X\Phi X^T$ with $i \in \{1,2\}$, and $Y = KX$, then one can pre- and post-multiplying both side of left equalities in (13) with $diag[X, XX, X, I, X, X]$ and right inequalities in (13) with $diag[X, X]$. By using $-X\overline{R}_iX \le \overline{R}_i - 2X$ to deal with the nonlinear terms in (13).

Remark 6 *Different from the controller synthesis proposed in[27,30,34], the controller design not only depended on the parameter σ_ϵ but also the parameter ϵ. By introducing the parameter ϵ, an upper bound of the event threshold is well given. Then, the designed controller K according to both σ_ϵ and ϵ can be well used to cope with the fluctuation of the event-triggered threshold. This is very different from the above controller design with a fixed event-triggered threshold.*

Moving forward, the co-design algorithm for finding the event-triggered parameter σ_ϵ is presented.

Algorithm 1 Co-design of control and communication

1: Set the positive scalars ϵ, τ_m, τ_M ($\tau_m \le \tau_M$), α, ς and the initial event triggered parameter σ_ϵ. Give the increasing step $\Delta > 0$ and an optimization target $topt < 0$;
2: While $topt < 0$
3: $\sigma_\epsilon = \sigma_\epsilon + \Delta$
4: Solve LMIs (14), if there is a feasible solution P, Q_i, R_i ($i = 1,2$) and Φ satisfying LMIs (14), go to the next step. Otherwise, return *Step 1*.
5: Return $\sigma_\epsilon - \Delta$ and calculate K and Φ.

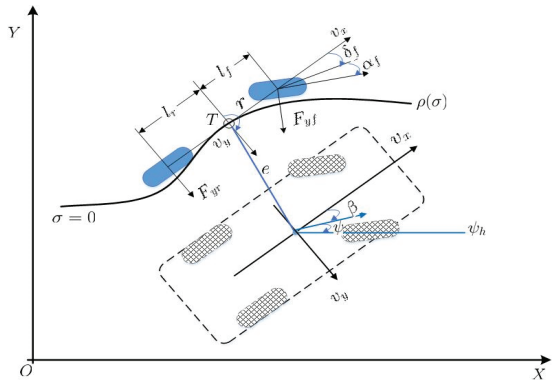

Figure 3. Kinematics model of path following control.

4. VERIFICATION EXAMPLES

In this section, simulation results are provided to verify the designed stabilization method under the SS-ETC scheme for path following control of AGVs. The kinematics model of AGVs is depicted in Figure 3, and the detailed parameters can be browed from [32] with $m = 1500kg$, $I_z = 2500kg \cdot m^2$, $l_s = 0.8m$, $l_f = 1.3m$, $l_r = 1.4m$, $C_f = 40000N/rad$, $C_r = 40000N/rad$, $v_x = 25km/h$.
The initial state is given by $x(0) = \begin{bmatrix} -0.1 & 0 & -0.01 & 0.2 \end{bmatrix}$, the external disturbance is $w(t) = 0.01\sin(t)$ during $t \in [30s, 45s]$.

Let $\tau_m = 0.1$, $\tau_M = 0.2$, $\alpha = 0.32$, $\epsilon = 1$. For comparisons, the controller's gain K_0 based on time delay method is given by

$$K_0 = \begin{bmatrix} -0.006 & -0.136 & -0.036 & -0.0408 \end{bmatrix} \tag{15}$$

Then according to Algorithm 1 and by solving LMIs (13) in Theorem 2, the controller gain for SS-ETC is obtained that $\sigma_\epsilon = 0.23$ and

$$K_1 = \begin{bmatrix} -0.001 & -0.0806 & -0.0202 & -0.0254 \end{bmatrix} \tag{16}$$

with

$$\Phi = 10^8 \times \begin{bmatrix} 1.7610 & -0.0237 & -0.1534 & 0.1880 \\ -0.0237 & 0.2489 & -0.4727 & -0.4127 \\ -0.1534 & -0.4727 & 0.9203 & 0.7671 \\ 0.1880 & -0.4127 & 0.7671 & 0.6969 \end{bmatrix}.$$

By setting sampling period $h = 0.1s$ and simulation length $T = 150s$, the following simulation results for comparisons are obtained.

Firstly, the state responses of the path following control are compared under a time-triggered scheme, static ETC scheme, and SS-ETC scheme, respectively. The simulations are given as follows. From the above simulation results from Figure 4 ~ Figure 7, the control performances, which include convergence and stability prosperities, are indeed improved under the proposed SS-ETC scheme by comparing with static ETC scheme.

Then, we will observe the control performance with the given index $J = ||x(t)||^2$. The detailed performances are given in Table 2.

Table 2 shows that the control performance under SS-ETC is still less than a time-triggered control scheme. This implies that the functional safety is well trade-off between the time-triggered control scheme and static ETC scheme when the SS-ETC scheme is adopted.

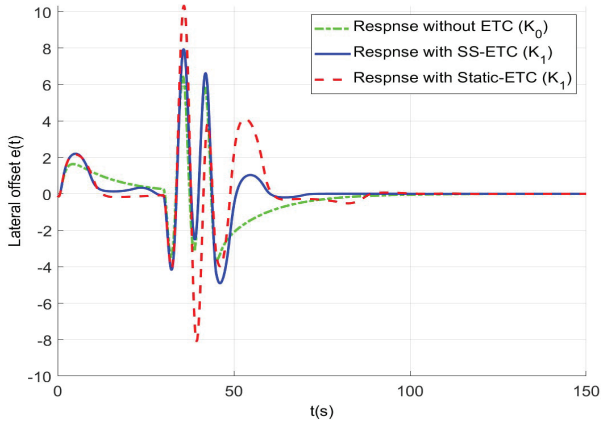

Figure 4. Response of lateral offset.

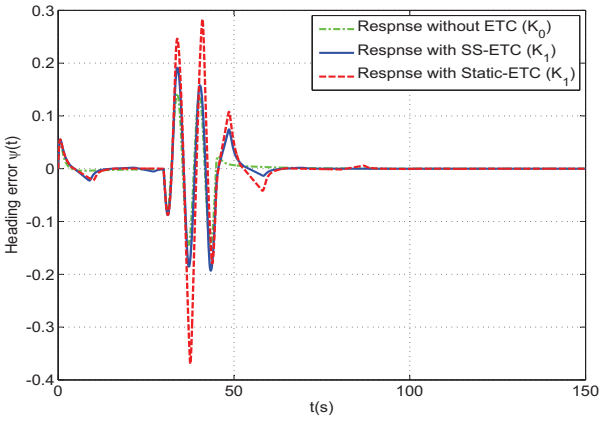

Figure 5. Comparisons of heading error response.

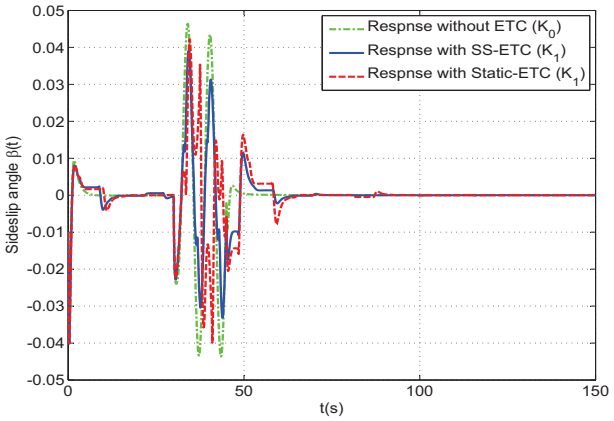

Figure 6. Comparisons of sideslip angle response.

Following this, we will analyze communication behaviors for the time-triggered transmission scheme, static

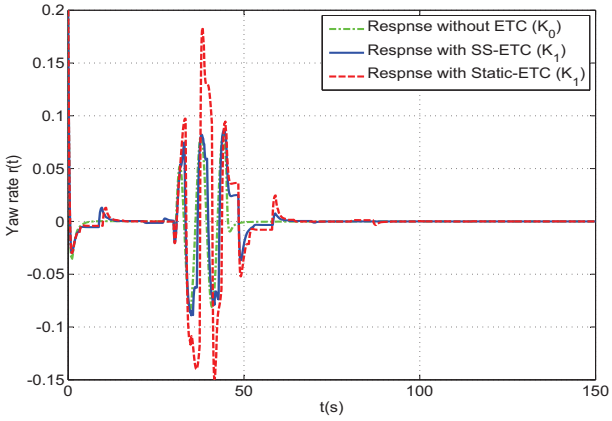

Figure 7. Comparisons of yaw rate response.

Table 2. Performance comparisons

J_0 with period transmission	J_1 with static ETC	J_2 with SS-ETC
2.7420×10^3	5.6193×10^3	3.6061×10^3

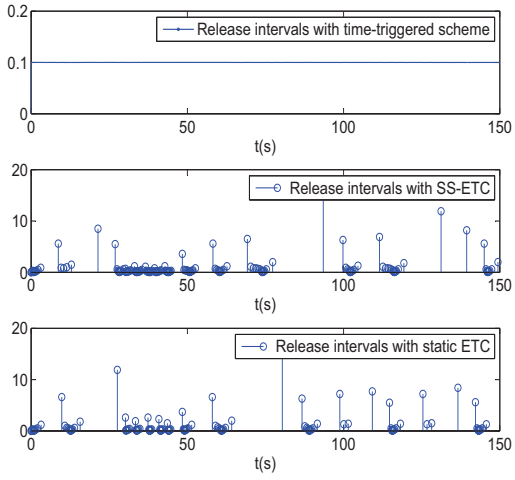

Figure 8. Release interval comparisons.

Table 3. Transmission comparisons

Time-triggered scheme		Static ETC scheme		SS-ETC scheme	
Transmission times	Average period	Transmission times	Average period	Transmission times	Average period
1500	0.1	133	1.0955	179	0.8346

ETC scheme, and SS-ETC scheme.

Based on Figure 8, the transmission times and average periods are given below. From Figure 8 and Table 3,

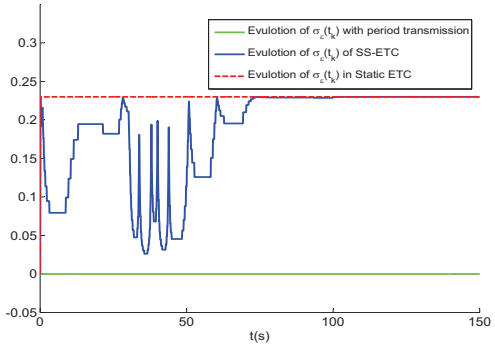

Figure 9. Evolutions of threshold comparisons.

one can see that the transmission times of SS-ETC are more than the ones of static ETC, and a less average transmission period is achieved. However, it is still far less than the time-triggered scheme. This is the reason why the SS-ETC can improve the control performance while saving communication resources. Nevertheless, such extra transmissions are based on the perception of the physical systems.

In order to present the evolutions of the SS-ETC scheme, the following simulation is used to record the change of event-triggered thresholds of the SS-ETC.

The adaptiveness of the proposed SS-ETC scheme is shown in Figure 9, where the event-triggered threshold would be dynamically adjusted according to the state measurement in real time. Recalling (5), when $||x(t_k h)||$ becomes a larger one; thus a smaller event threshold is adopted. This is helpful in improving control performance when an unstable measurement is detected. However, the threshold is equal to the static event-triggered parameter when the state measurement $||x(t_k h)|| \to 0$. This is helpful in reducing transmissions when the system is stable.

From the above simulation results, we can arrive at the following facts.

- If $||x(t_k h)|| \to 0$, the event-triggered parameter in the SS-ETC scheme will degenerate to the static event-triggered parameter, which is beneficial to reduce transmissions when a stable measurement is observed.
- An adaptive adjustment scheme of the proposed SS-ETC is sensitive to fluctuations in measurements. Once an unstable state measurement is detected, the SS-ETC scheme will adopt a smaller event-triggered threshold to encourage a transmission, where better control performance is expected.
- Under the proposed SS-ETC scheme, the control performance can be well improved, even at the cost of increased communication consumption. This supplies a dynamic way to trade off between control and communication.

Under the above discussions, the proposed SS-ETC scheme provides a more flexible transmission way to accommodate control requirements.

5. CONCLUSIONS

So far, a novel SS-ETC scheme has been well designed for reducing communication load while ISS is achieved. The barrier-like function is first introduced to design such a SS-based ETC scheme. The proposed SS-ETC scheme shows some intelligent features when adjusting the event-triggered threshold by a nonlinear function. The intelligence of the proposed SS-ETC scheme can be summarized as follows:

- The event thresholds of such sampled-data error will be suppressed in a given upper bound, which the

stability of the NCS is guaranteed;
- The event thresholds realize the two-way adjustment (decrement and increment) according to the state measurement automatically.

Under the proposed SS-ETC, the networked path following model, which included both communication and control parts, has been accurately described. Then, the stability analysis and controller design have been derived in detail for the purpose of ISS. At last, some simulation experiments have been conducted to confirm the effectiveness of the proposed co-design method for SS-ETC. Different from the previous works on variable-threshold ETC, the designed SS-ETC adjusted event threshold solely based on the physical state perception. In fact, the proposed SS-ETC is a class of state-oriented communication schemes in which the physical security of path following control can be well guaranteed.

However, the proposed SS-ETC scheme failed to discuss the following aspects.

- It is obvious that the parameter ϵ will make any difference on the event-triggered condition. How to design such a parameter is not included in this paper;
- So far, the proposed SS-ETC scheme only depended on state measurement. Some other more reasonable indexes should be further considered;
- In fact, if the vehicle maneuvers very fast, the nonlinear dynamics of the vehicle is not negligible, and a linear controller is not effective. Therefore, the controller design by considering nonlinear dynamics of the vehicles should be included;
- In addition, due to vulnerability of communication networks, a security SS-ETC scheme, which includes both physical state and communication security perception, is still a challenging problem [35,36].

The above issues may be left for our future work.

DECLARATIONS

Authors' contributions

Conception and design of the study: Sun HT
Administrative support: Huang J
Data analysis and interpretation: Chen Z, Wang Z

Availability of data and materials

Not applicable.

Financial support and sponsorship

This work was supported in part by the National Natural Science Foundation of China under Grants 62103229, 62263019, the Natural Science Foundation of Shandong Province under Grant ZR2021QF026, the China Postdoctoral Science Foundation under Grant 2021M692024, the National Key R & D Program of China under Grant 2021YFE0193900.

Conflicts of interest

All authors declared that there are no conflicts of interest.

Ethical approval and consent to participate

Not applicable.

Consent for publication

Not applicable.

REFERENCES

1. Wang H, Zhao H, Zhang J, Ma D, Li J, Wei J. Survey on unmanned aerial vehicle networks: a cyber physical system perspective. *IEEE Commun Surv Tutorials* 2020;22:1027-70. DOI
2. Yurtsever E, Lambert J, Carballo A, Takeda K. A survey of autonomous driving: Common practices and emerging technologies. *IEEE Access* 2020;8:58443-69. DOI
3. Shojaei K, Yousefi MR. Tracking control of a convoy of autonomous robotic cars with a prescribed performance. *T I Meas Control* 2019;41:3725-41. DOI
4. Mezair T, Djenouri Y, Belhadi A, Srivastava G, Lin JC. Towards an advanced deep learning for the internet of behaviors: Application to connected vehicles. *ACM Trans Sen Netw* 2023;19:1-18 DOI
5. Ni J, Hu J, Xiang C. Robust control in diagonal move steer mode and experiment on an X-by-wire UGV. *EEE/ASME Trans Mechatron* 2019;24:572-84. DOI
6. Gu Z, Yin T, Ding Z. Path tracking control of autonomous vehicles subject to deception attacks via a learning-based event-triggered mechanism. *IEEE Trans Neural Netw Learn Syst* 2021;32:5644-53. DOI
7. Shuai Z, Zhang H, Wang J, Li J, Ouyang M. Combined AFS and DYC control of four-wheel-independent-drive electric vehicles over can network with time-varying delays. *IEEE Trans Veh Technol*2014;63:591-602. DOI
8. Wang Z, Li G, Jiang H, Chen Q, Zhang H. Collision-free navigation of autonomous vehicles using convex quadratic programming-based model predictive control. *IEEE/ASME Trans Mechatron* 2018;23:1103-13. DOI
9. Chang X, Liu Y, Shen M. Resilient control design for lateral motion regulation of intelligent vehicle. *IEEE/ASME Trans Mechatron* 2019;24:2488-97. DOI
10. Shin J, Kwak D, Lee T. Robust path control for an autonomous ground vehicle in rough terrain. *Control Eng Pract* 2020;98:104384. DOI
11. Wu Y, Wang L, Zhang J, Li F. Path following control of autonomous ground vehicle based on nonsingular terminal sliding mode and active disturbance rejection control. *IEEE Trans Veh Technol* 2019;68:6379-90. DOI
12. Ni J, Hu J. Dynamics control of autonomous vehicle at driving limits and experiment on an autonomous formula racing car. *Mech Syst Signal Process* 2017;90:154-74. DOI
13. Chen T, Cai Y, Chen L, Xu X, Sun X. Trajectory tracking control of steer-by-wire autonomous ground vehicle considering the complete failure of vehicle steering motor. *Simul Model Pract and Theory* 2021;109:102235. DOI
14. Hu C, Chen Y, Wang J. Fuzzy observer-based transitional path-tracking control for autonomous vehicles. *IEEE Trans Intell Transport Syst* 2021;22:3078-88. DOI
15. Chen D, Liu G. Coordinated path-following control for multiple autonomous vehicles with communication time delays. *IEEE Trans Contr Syst Technol* 2020;28:2005-12. DOI
16. Wang H, Song W, Liang Y, Li Q, Liang D. Observer-based finite frequency h_∞ state-feedback control for autonomous ground vehicles. *ISA Trans* 2022;121:75-85. DOI
17. Shojaei K. Neural adaptive pid formation control of car-like mobile robots without velocity measurements. *Advanced Robotics* 2017;31:947-64. DOI
18. Guo G, Wen S. Communication scheduling and control of a platoon of vehicles in vanets. *Trans Intell Transport Syst* 2016;17:1551-63. DOI
19. Gu Z, Yin T, Ding Z. Path tracking control of autonomous vehicles subject to deception attacks via a learning-based event-triggered mechanism. *IEEE Trans Neural Netw Learn Syst* 2021;32:5644-53. DOI
20. Li W, Xie Z, Wong PK, Mei X, Zhao J. Adaptive-event-trigger-based fuzzy nonlinear lateral dynamic control for autonomous electric vehicles under insecure communication networks. *IEEE Trans Ind Electron* 2021;68:2447-59. DOI
21. Zhang G, Chu S, Jin X, Zhang W. Composite neural learning fault-tolerant control for underactuated vehicles with event-triggered input. *IEEE Trans Cybern* 2021;51:2327-38. DOI
22. Xie X, Zhou Q, Yue D, Li H. Relaxed control design of discrete-time takagi-sugeno fuzzy systems: an event-triggered real-time scheduling approach. *IEEE Trans Syst Man Cybern, Syst* 2018;48:2251-62. DOI
23. Zhang X, Han Q, Zhang B. An overview and deep investigation on sampled-data-based event-triggered control and filtering for networked systems. *IEEE Trans Ind Inf* 2017;13:4-16. DOI
24. Ge X, Han Q, Ding L, Wang Y, Zhang X. Dynamic event-triggered distributed coordination control and its applications: a survey of trends and techniques. *IEEE Trans Syst Man Cybern, Syst* 2020;50:3112-25. DOI
25. Peng C, Zhang J, Yan H. Adaptive event-triggering H_∞ load frequency control for network-based power systems. *IEEE Trans Ind Electron* 2018;65:1685-94. DOI
26. Girard A. Dynamic triggering mechanisms for event-triggered control. *IEEE Trans Automat Contr* 2015;60:1992-7. DOI
27. Hu S, Yue D, Xie X, Chen X, Yin X. Resilient event-triggered controller synthesis of networked control systems under periodic DoS jamming attacks. *IEEE Trans Cybern* 2019;49:4271-81. DOI
28. Xu W, Ho DWC, Zhong J, Chen B. Event/self-triggered control for leader-following consensus over unreliable network with dos attacks. *IEEE Trans Neural Netw Learn Syst* 2019;30:3137-49. DOI

29. Tian E, Peng C. Memory-based event-triggering H_∞ load frequency control for power systems under deception attacks. *IEEE Trans Cybern* 2020;50:4610-8. DOI
30. Peng C, Yang TC Event-triggered communication and H_∞ control co-design for networked control systems. *Automatica* 2013;49:1326-32. DOI
31. Zhou W, Fu J, Yan H, Du X, Wang Y, Zhou H. Event-triggered approximate optimal path-following control for unmanned surface vehicles with state constraints. *IEEE Trans Neural Netw Learn Syst* 2023;34:104-18. DOI
32. Wang R, Jing H, Hu C, Yan F, Chen N. Robust H_∞ path following control for autonomous ground vehicles with delay and data dropout. *IEEE Trans Intell Transport Syst* 2016;17:2042-50. DOI
33. Han Q. Absolute stability of time-delay systems with sector-bounded nonlinearity. *Automatica* 2005;41:2171-6. DOI
34. Zhang X, Han Q. Event-triggered dynamic output feedback control for networked control systems. *IET Control Theory A* 2014;8:226-34. DOI
35. Peng C, Sun H. Switching-like event-triggered control for networked control systems under malicious denial of service attacks. *IEEE Trans Automat Contr* 2020;65:3943-9. DOI
36. Sun H, Peng C. Event-triggered adaptive security path following control for unmanned ground vehicles under sensor attacks. *IEEE T Veh Tech* 2023. DOI

APPENDIX

Proof of Theorem 1: The following Lyapunov-Krasovskii functions are well constructed

$$V(t) = V_P(t) + V_{Q_1}(t) + V_{Q_2}(t) + V_{R_1}(t) + V_{R_2}(t)] \tag{17}$$

where

$$V_P(t) = x^T(t)Px(t)$$

$$V_{Q_1}(t) = \int_{t-\tau_m}^{t} e^{2\alpha(s-t)}x^T(s)Q_1x(s)ds$$

$$V_{Q_2}(t) = \int_{t-\tau_M}^{t-\tau_m} e^{2\alpha(s-t)}x^T(s)Q_2x(s)ds$$

$$V_{R_1}(t) = \tau_m \int_{-\tau_m}^{0}\int_{t+\theta}^{t} e^{2\alpha(s-t)}\dot{x}^T(s)R_1\dot{x}(s)dsd\theta$$

$$V_{R_2}(t) = (\tau_M - \tau_m)\int_{-\tau_M}^{-\tau_m}\int_{t+\theta}^{t} e^{2\alpha(s-t)}\dot{x}^T(s)R_2\dot{x}(s)dsd\theta$$

By differentiating the above designed functionals along with $x(t)$, we can obtain

$$\begin{aligned}\dot{V}_P(t) = {} & 2x^T(t)P[Ax(t) + BKx(t-\tau(t)) \\ & - BK\varsigma(i_k h) + Fw(t)]\end{aligned} \tag{18}$$

$$\begin{aligned}\dot{V}_{Q_1}(t) = {} & -2\alpha V_{Q_1}(t) + x^T(t)Q_1x(t) \\ & - e^{-2\alpha\tau_m}x^T(t-\tau_m)Q_1x(t-\tau_m)\end{aligned} \tag{19}$$

$$\begin{aligned}\dot{V}_{Q_2}(t) = {} & -2\alpha V_{Q_2}(t) + e^{-2\alpha\tau_m}x^T(t-\tau_m)Q_2x(t-\tau_m) \\ & - e^{-2\alpha\tau_M}x^T(t-\tau_M)Q_2x(t-\tau_M)\end{aligned} \tag{20}$$

$$\begin{aligned}\dot{V}_{R_1}(t) = {} & -2\alpha V_{R_1}(t) + \tau_m^2\dot{x}^T(t)R_1\dot{x}(t) \\ & - \tau_m\int_{t-\tau_m}^{t} e^{2\alpha(s-t)}\dot{x}^T(s)R_1\dot{x}(s)ds\end{aligned} \tag{21}$$

$$\dot{V}_{R_2}(t) = -2\alpha V_{R_2}(t) + (\tau_M - \tau_m)^2 \dot{x}^T(t) R_2 \dot{x}(t) - (\tau_M - \tau_m) \int_{t-\tau_M}^{t-\tau_m} e^{2\alpha(s-t)} \dot{x}^T(s) R_2 \dot{x}(s) ds \tag{22}$$

In view of Lemma 1 and Lemma 2, the following relation holds

$$-\tau_m \int_{t-\tau_m}^{t} e^{2\alpha(s-t)} \dot{x}^T(s) R_1 \dot{x}(s) ds \leq -e^{-2\alpha\tau_m} \begin{bmatrix} x(t) \\ x(t-\tau_m) \end{bmatrix}^T \begin{bmatrix} R_1 & -R_1 \\ -R_1 & R_1 \end{bmatrix} \begin{bmatrix} x(t) \\ x(t-\tau_m) \end{bmatrix} \tag{23}$$

and

$$-(\tau_M - \tau_m) \int_{t-\tau_M}^{t-\tau_m} e^{2\alpha(s-t)} \dot{x}^T(s) R_2 \dot{x}(s) ds \leq -e^{-2\alpha\tau_M} \zeta^T(t) \begin{bmatrix} R_2 & S - R_2 & -S \\ * & 2R_2 - S - S^T & S - R_2 \\ * & * & R_2 \end{bmatrix} \zeta(t) \tag{24}$$

where $\zeta^T = \begin{bmatrix} x(t-\tau_m) & x(t-\tau(t)) & x(t-\tau_M) \end{bmatrix}$.

By summing up (18) ~ (24) and applying $\varsigma^T(i_k h)\Phi\varsigma(i_k h) \leq \frac{\sigma_\epsilon}{\epsilon}\mathcal{X}(t_k)$, the following relation is achieved

$$\dot{V}(t) + 2\alpha V(t) - \varsigma w^T(t) w(t) < \chi^T(t)\Pi_{11}\chi(t) + \tau_m^2 \dot{x}^T R_1 \dot{x} + (\tau_M - \tau_m)^2 \dot{x}^T R_2 \dot{x} \tag{25}$$

where $\chi(t) = col\{x(t), x(t-\tau_m), x(t-\tau(t)), x(t-\tau_M), w(t)\}$ and Π_{11} is given in (13).

Using Schur complement for (25), (13) hold when $\Pi < 0$ for all t.

Let $a = \lambda_{min}(P)$, $b = \lambda_{max}(P) + \eta_2\lambda_{max}(Q_i) + \frac{\eta_2^2}{2}\lambda_{max}(R_i)$ and $||\overline{w}|| = \max(||w(t)||)$ for $i = 1, 2$, it gives

$$||x(t)|| \leq \sqrt{\frac{b}{a}} e^{-\alpha t} ||x(0)|| + \varsigma\sqrt{\frac{1}{a}} ||\overline{w}|| \tag{26}$$

from (25).

Obviously, (26) shows that the NCS (9) is ISS under the SS-ETC scheme (5).